NJC

Accepted Manuscript

This is an *Accepted Manuscript*, which has been through the Royal Society of Chemistry peer review process and has been accepted for publication.

Accepted Manuscripts are published online shortly after acceptance, before technical editing, formatting and proof reading. Using this free service, authors can make their results available to the community, in citable form, before we publish the edited article. We will replace this *Accepted Manuscript* with the edited and formatted *Advance Article* as soon as it is available.

You can find more information about *Accepted Manuscripts* in the Information for Authors.

Please note that technical editing may introduce minor changes to the text and/or graphics, which may alter content. The journal's standard Terms & Conditions and the Ethical guidelines still apply. In no event shall the Royal Society of Chemistry be held responsible for any errors or omissions in this *Accepted Manuscript* or any consequences arising from the use of any information it contains.

ROYAL SOCIETY OF CHEMISTRY

www.rsc.org/njc

Journal Name

RSCPublishing

ARTICLE

TiO_2 Hollow Nanocrystals Through the Nanoscale Kirkendall Effect for Lithium-ion Batteries and photocatalysis

Cite this: DOI: 10.1039/xoxxooooox

Jicai Liang [a], Xiangbo Han[a], Yi Li [a], Kaiqi Ye[b], Changmin Hou[c] and Kaifeng Yu[a*]

Received ooth January 2012,
Accepted ooth January 2012

DOI: 10.1039/xoxxooooox

www.rsc.org/

TiO_2 Hollow structures have important applications in high performance lithium ion batteries and efficient photocatalysis. In contrast to the conventional synthesis routes where various soft or hard templates are usually put into use, the direct growth of uniform TiO_2 Hollow nanocrystals is presented. The growth mechanism, lithium ion battery performance, and photocatalytic activity of the resultant TiO_2 hollow nanocrystals are thoroughly investigated. TiO_2 hollow nanocrystals can be synthesized through a mechanism analogous to the nanoscale Kikendal Effect. The hollow structure results in highly active photocatalysis, a high rate capability, and stable cycling.

1. Introduction

Inorganic hollow structures have attracted increasing research interest because of their intriguing properties and numerous potential applications as catalysts, lightweight fillers, low-dielectric materials, drug-release vectors, photonic crystals, and others.[1] Researchers have developed various strategies to controllably synthesize different hollow structures for many materials.[2] Recently, some novel methods have been developed to synthesize various hollow nano/microspheres such as templating methodologies,[3] surface-protected etching,[4] Ostwald Ripening,[5] Kirkendall effect,[6] and so on. Among them, the nanoscale Kirkendall effect is a classical phenomenon in metallurgy, which normally refers to a nonequilibrium mutual diffusion process through the interface of coupled materials, and to obtain the very good application in synthesis of hollow nanostructures.[7] Predecessors have put to use the method based on the nanoscale Kirkendall effect to prepare a lot of kinds of hollow nanostructures. For example, Cabot et al. reported asymmetric Cd/CdS partial hollow nanospheres;[8] Tang et al. reported the formation of Ag_2Se hollow nanocrystals;[9] Chiang et al. reported the synthesis of Ni_2P hollow nanocrystals through nanoscale;[10] Wang et al. also reported the formation of Ni_2P/Ni_2P_5 hollow nanocrystals,[11] etc.

Due to its peculiar chemical and physical properties, titanium dioxide (TiO_2) as an important semiconductor has been investigated extensively for a vast range of applications (e.g., photocatalysis, solar cells/batteries, field emission, and self-cleaning).[12] Recently, major research appears to be shifting to create TiO_2 hollow structure, because they have been evaluated as attractive candidates for sensors, lithium storage, lithium-ion batteries, solar cells, and photocatalysts.[12b,13]

As a result, TiO_2 hollow nanocrystals whose scale is less than 20 nm is not reported. The cushy synthesis of high quality TiO_2 hollow nanocrystals is seldom reported, despite the fact that numberous TiO_2 hollow nanostructures have been reported by different templating of template-free methods. To develop simple and scalable strategies for the synthesis of TiO_2 hollow nanocrystals is thus highly desirable and technologically important.

Herein, we report a simple nanoscale Kirkendall effect method to synthesize TiO_2 hollow nanocrystals. The fabrication process is low-cost, convenient and scalable, while the produced TiO_2 hollow nanocrystals exhibit excellent electrochemical and photochemical properties. The small size and high crystallinity of primary TiO_2 nanoparticles and the high structural integrality of the TiO_2 hollow nanocrystals give rise to significant improvements in the cycling stability, rate performance and photocatalytic performance of the TiO_2 hollow nanocrystals.

2. Results and Discussion

2.1 The formation mechanism of TiO_2 hollow nanocrystlas

The formation mechanism of TiO_2 hollow nanocrystlas may relate to the nanoscale Kirkendall effect.[14] In 1947, Smigelskas and Kirkendall repeated the Kirkendall effect that was the first experimental proof that atomic diffusion occurs through vacancy exchange and not by the direct interchange of atoms.[15] In 2004, Yadong Yin et al. reported that hollow nanocrystals were synthesized by nanoscale Kirkendall effect for the first time.[14] The synthesis of TiO_2 hollow nanocrystals is simple and straightforward, as illustrated in Figure 1. For nanoscale Kirkendal effect in a nanocrystal solution system, the formation of TiO_2 hollow nanocrystals is a one-pot, two-step process. The first step involves the formation of vacancies in TiO_2 nanocrystals because of the surface-to-volume ratio of the particle and the absence of defects in the TiO_2 nanocrystals. The next step, within the small volume of a transforming nanocrystal, the supersaturated vacancy cloud is likely to amalgamate into a single void. During the second step, the core/shell structure will be usually produced. The direct conversion of core material to shell material is therefore hindered by the layer and further reaction will continue by the diffusion of atoms or ions

through the interface. If the diffusion rate of core material is faster than that of shell material, the preferred outward diffusion of atoms or ions from core to shell leads to a net material flux across the nanocrystal interface and simultaneously results in a flow of fast-moving vacancies to the vicinity of the solid-liqiud interface. Therefore, the hollow voids are formed through coalescence of the vacancies based on nanoscale Kirkendall effect. Adopting such high quality TiO_2 nanocrystals as the starting materials, it should be possible to produce a relatively uniform population of TiO_2 hollow nanocrystals.

2.2 The structure of TiO_2 hollow nanocrystlas

The crystal structure of the samples was characterized by using X-ray diffraction. Figure S1a shows representative powder XRD patterns of the samples at various hydrothermal times. The diffraction peaks can be indexed to anatase TiO_2 (JCPDS No. 21-1272)[16] and monoclinic metastable polymorph of TiO_2(B) (space group C2/m, JCPD No. 35-0088).[17] The framework of the TiO_2(B) structure is constructed from corrugated sheets of edge and corner-sharing TiO_6 octahedra that are linked by bridging oxygen atoms to form a three-dimensional network. This structure is more open than those of rutile and anatase, consequently making the material an effective host for lithium ion storage.[18] TiO_2 hollow nanocrystals show a relatively high Brunauer-Emmett-Teller (BET) specific surface area of 133 m^2g^{-1} (N2 adsorption –desorption isotherms are given in Figure S1b). The plots of pore size distribution are calculated from the desorption isotherm using the Saito-Foley (SF statistical micropore<2nm) and Barrett–Joyner–Halenda (BJH statistical mesoporous) model. Figure S1b shows TiO_2-48h hollow nanocrystals possess the microporous and mesoporous structure.

The morphological characterizations of TiO_2 hollow nanocrystals are shown in Figure 2. The sample (TiO_2-48h) showed in Figure 2b has good dispersion and no agglomeration. The diameter of TiO_2 hollow nanocrystals is about 15 nm, and the wall thickness of hollow nanocrystals is about 2 to 5 nm. The samples showed in Figure 2a (TiO_2-24h) and Figure 2c (TiO_2-72h) have a certain degree of reunion phenomenon. As showed in Figure 2a, some nanocrystals also stick together. As showed in Figure 2c, there are some lamellae in addition to a number of hollow nanocrystals. Figure 2d (TiO_2-24h), 2e (TiO_2-48h), and 2f (TiO_2-72h) show the SAED patterns of the samples. The SAED patterns of the TiO_2 hollow nanocrystals indicate the polycrystalline nature of the samples and each of the diffraction rings can be indexed readily to anatase TiO_2 and TiO_2(B), which is consistent with the XRD results.

The microstructure of TiO_2 hollow nanocrystals is further analyzed by high-resolution TEM (HRTEM). Figure S2 shows the HRTEM images of TiO_2-48h hollow nanocrystals. As showed in Figure S2a and Figure S2b, the diameter of TiO_2 hollow nanocrystals s is about 15 nm and the wall thickness of diameter approximately 2 to 5 nm. As showed in Figure S2c and Figure S2d, the interplanar distance between the lattice fringes is measured to be 0.35 and 0.62 nm, which can be indexed to (101) and (001) crystal planes of anatase TiO_2 and TiO_2(B). It is consistent with the XRD results.

The hollow structure, microporous and mesoporous structure, and high specific surface area features of the TiO_2 hollow nanocrystals are attractive characteristics in a large range of applications such as catalysis and energy conversion and storage. In this work, we evaluate the electrochemical performance and photocatalysis of the TiO_2 hollow nanocrystals as anodes for lithium ion batteries and photocatalyst.

2.3 The application of TiO_2 hollow nanocrystlas for Lithium-ion Batteries and photocatalysis

To corroborate the advantages of the TiO_2 hollow nanocrystals, we have appraised their lithium storage properties as anode materials for LIBs. The cyclic voltammograms of three samples (Figure S3) exhibit basic symmetry oxidation and reduction peaks. It exhibit that there is few irreversible capacity loss in TiO_2 hollow nanocrystals. Figure S4 displays the rate performance of TiO_2-24h, TiO_2-48h, TiO_2-72h at charge/discharge rate at 0.5 C, 1 C and 2 C. At each stage, TiO_2-48 is significantly higher than the TiO_2-24h and TiO_2-72h. Figure 3a shows the cycling performance of TiO_2 hollow nanocrystals at a current density of 0.5 C (1 C=168 mAg^{-1}) voltage profiles within a cut-off voltage window of 1.0–2.5 V. The discharge specific capacity and cycle stability of TiO_2-48h are better than that of TiO_2-24h and TiO_2-72h. Figure 3b shows representative discharge–charge voltage profiles within a cut-off voltage window of 1.0–2.5 V versus Li^+/Li, respectively, which correspond to the lithium insertion/de-insertion process.[19] All electrodes display discharge curve of smooth slopes between 1.3 V and 1.8 V, the other one, charging curve of two smooth slopes between 1.4 V and 2.0 V. It is different from the characteristic charge-discharge plateaus atw1.7 V and 1.9V for anatase TiO_2. This is due to the different Li^+ ion intercalation mechanisms between TiO_2(B) and anatase. It has been identified that the Li^+ ion intercalation into TiO_2(B) is a pseudocapacitive faradic process, rather different from the solid-state diffusion process observed for anatase.[18a, 20] Moreover, the TiO_2 hollow nanocrystals exhibit excellent rate capability at discharge-charge current rates ranging from 0.5C to 10C, as shown in Figure 3c. The first discharge capacities are 323 mAg^{-1} for the TiO_2-48, 299.4 mAg^{-1} for the TiO_2-24h, 234.5 mAg^{-1} for the TiO_2-72h in 0.5 C of ratio, respectively. The discharge specific capacity of TiO_2-48h sample is 205.3 $mAhg^{-1}$ after 90 cycles at the 0.5C ratio. After the high-rate discharge–charge cycling, a specific capacity of TiO_2-48h (231.6 $mAhg^{-1}$) can be restored when the current density is decreased to 0.5 C. TiO_2-48h hollow nancrystals have high specific capacity and good cycle stability (Figure S5). The electrode of TiO_2-48h hollow nancrystals yields the first charge capacity of 182 $mAhg^{-1}$, 166.1 $mAhg^{-1}$ and the discharge capacity of 237.6 $mAhg^{-1}$, 220.2 $mAhg^{-1}$ for the 10C and 20C. These results clearly demonstrate the superior lithium storage properties of TiO_2 Hollow Nanocrystals in terms of long cycle life and a good rate capability for the fast charging/discharging process.

The outstanding electrochemical performance of the as-prepared TiO_2 hollow nanocrystals as anode materials for LIBs can be understood from several viewpoints. First, the cavities in the hollow structure may provide extra space for the storage of lithium ions, which is beneficial for enhancing specific capacity of the battery.Second, the hollow structure with high surface area provides more active surface locations and electo-lyte-electrode interface compared with solid materials. Third, the small size of the nanocrystals and the relatively thin shell offer a shortly diffusive distance for lithium ions, thus elevating fast and reversible lithium insertion and extraction. Fourth, the shell structure with a nanometer size effectively prevents the undesirable aggregation of traditional nanomaterials, which insures the intactness of the electrode and improve the capacity retention upon agelong cycling. Fifth, the void space in hollow structures buffers against the local volume change during lithium insertion-deinsertion and is able to alleviate the problem of pulverization and aggregation of the electrode material, hence improving the cycling performance.The properties would elevate the electrochemical performance and lead to high specific capacity extraordinarily at high rates.

In addition to the high performance of LIBs, the TiO_2 hollow nanocrystals also enable the high photocatalytic activity. The photocatalytic activity of TiO_2 hollow nanocrystals and P25 were measured using a 500 W ultraviolet (UV) light lamp. The solution for photodegradation measurement were prepared by adding an amount of 20 mg of TiO_2 hollow nanocrystals to 20 mL of aqueous solution of methylene blue (MB, 20 mg/l). In order to ensure that the photocatalysts were well dispersed in the MB solution, the mixture s were initially treated with ultrasonic stirring for 3 min, followed by continuous stirring in the dark for 30 min to achieve an adsorption–desorption equilibrium. Figure 4 shows photocatalytic activities of TiO_2 hollow nanocrystals and P25 under UV light irradiation. The degradation of methylene blue has been completed within 40 minutes in the presence of TiO_2 hollow nanocrystals. A comparison of photocatalytic activity between TiO_2 hollow nanocrystals and P25 has been done to approach the advantage of TiO_2 hollow nanocrystals.

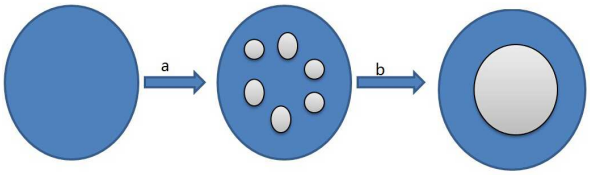

Figure 1. Schematic illustration of nanoscale Kirkendall effect for the formation of TiO_2 hollow nanocrystals.

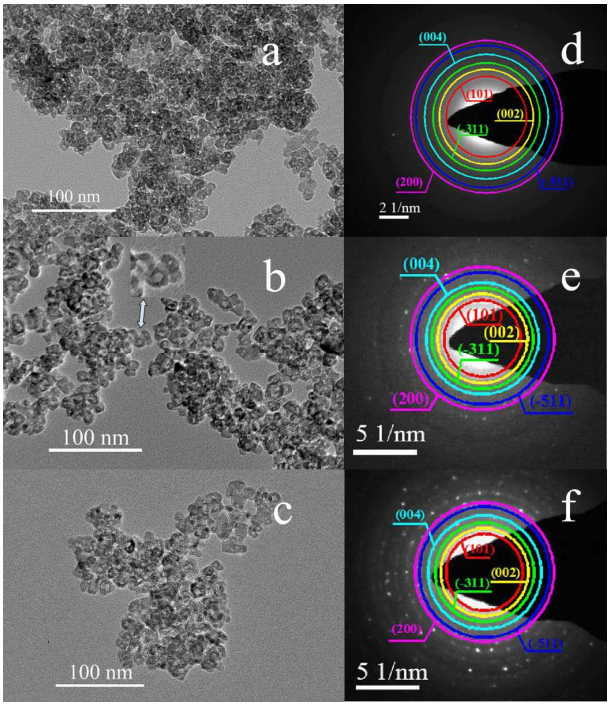

Figure 2. TEM and SAED images of TiO_2 hollow nanocrystals synthesized with different time: (a) and (d) 24 h; (b) and (e) 48 h; (c) and (f) 72 h.

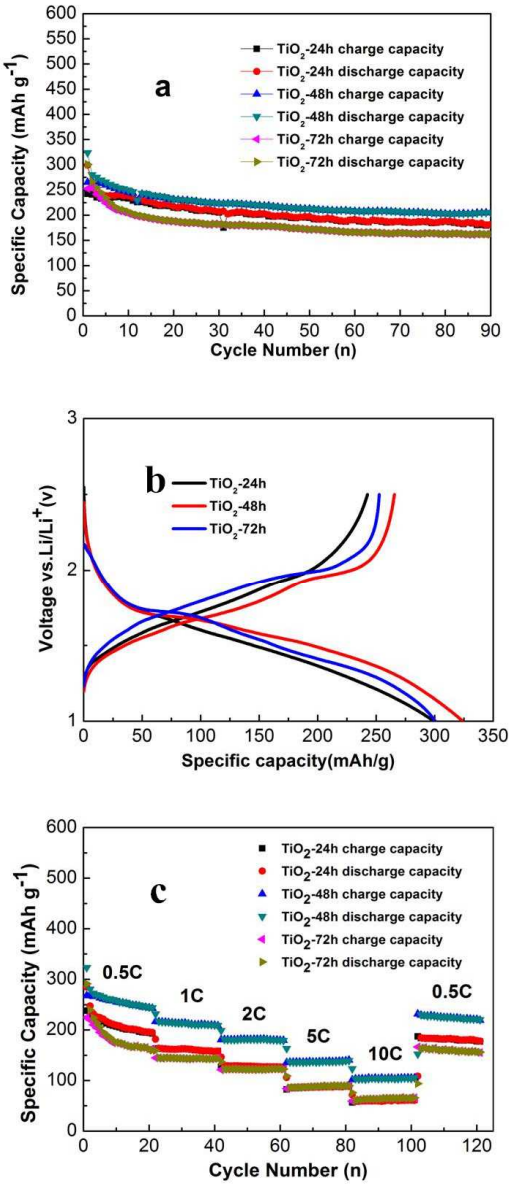

Figure 3. Electrochemical performance of TiO_2 hollow nanocrystals as an anode material in LIBs: a) Cycling performance of electrode at constant ratio of 0.5 C; b) The first charge−discharge voltage profiles at 0.5 C; c) Rate capability at various current fates from 0.5 C to 10 C for 20 cycles.

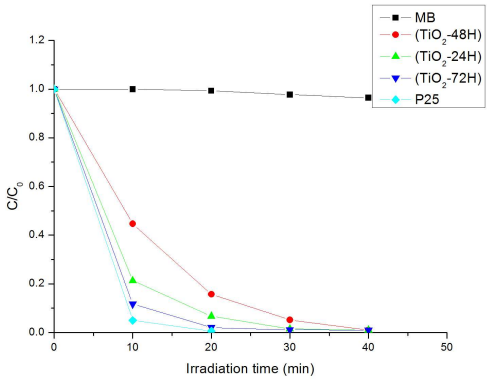

Figure 4. Photodegradation of MB for TiO_2 Hollow Nanocrystals under UV light irradiation.

3. Conclusions

In summary, we have developed a novel scalable route to prepare non-monolithic phase (anatase and TiO_2(B)) porous TiO_2 hollow nanocrystals by the hydrothermal reaction. Test results can be seen through this unique TiO_2 hollow nanocrystals, it exhibit good electrochemical performance with a high reversible capacity, long cycle life, rate performance, and its low cost, non-polluting, making it promising for the next generation Li ion batteries. Moreover, TiO_2 hollow nanocrystals have great potential application for air purification as the photocatalyst. We believe that the present synthetic route can be further extended to produce other in situ growth materials with promising applications for Lithium ion batteries and photocatalysis.

4. Experimental

Materials synthesis: In a typical synthesis, TiO_2 hollow nanocrystals were synthesized via a simple hydrothermal process. An aqueous solution of $Ti(SO4)_2$ was added in a vessel. NaOH solution was then added dropwise to the vessel under stirring at room temperature. Gelatinous white precipitate was formed instantly. The resulting precipitate was separated from the mother liquor by centrifugation and washed with distilled water until the absence of residual SO_4^{2-} (tested by the reaction of them with a $BaCl_2$ solution). Subsequently, further treatment with the 6.3g $LiOH{\cdot}H_2O$ and 30ml deionized water aqueous solution in a Teflon vessel at 130 ^oC was carried out for 24 h, 48 h and 72 h, respectively. After the hydrothermal treatment, the precipitates were separated by filtration and washed with diluted HCl solution and deionized water. At last, the samples were calcinated at 450 ^oC for 3 h.

Materials characterization: X-ray diffraction (XRD) patterns were collected on a Bruker D8 Advance X-ray Diffractometer. Transmission electron microscope (TEM) images were taken on a Tecnai G2 S-Twin F20 microscope. High resolution TEM (HRTEM) analysis was performed on a Tecnai G2 S-Twin F20 microscope.

Electrochemical measurements: the working electrode consisted of active material (i.e., hollow TiO_2 nanocrystals), Carbon black, and polymer binder (polyvinylidene fluodide, PVDF) in a weight ratio of 85:5:10. Lithium fiol was used as both the counter electrode and reference electrode. 1M LiPF6 in a 50:50 w/w mixture of ethylene carbonate and diethyl carbonate was used as the electrolyte. Cell assembly was carried out in an Ar-filled glovebox with misture and oxygen concentrations below 1.0 ppm. Cyclic voltammetry measurements were performed on a CHI660C electrochemical workstation. The galvanostatic charg-discharge tests were performed on a LAND(CT2001A)battery test system.

The photocatalytic activity of the sample was measured by monitoring the degradation of methylene blue (MB) at ambient temperature using a 500 W UV-violet light lamp, and the optical properties of the films were characterized by a UV–visible spectrophotometer (UV-6100PC).

Acknowledgements

The work is supported by the Key Scientific and Technological Project of Jilin Province, Project Grant No. 20140204052GX; Open Project of State Key Laboratory of Supramolecular Structure and Materials (sklssm201438); the State Key Laboratory of Inorganic Synthesis and Preparative Chemistry, College of Chemistry, Jilin University (No. 2013-27) and Science and Technology Development Program of Jilin Province (20120319).

Notes and references

[a]Key Laboratory of automobile Materials, Ministry of Education, and College of Materials Science and Engineering, Jilin University, Changchun 130025, China e-mail: yukf@jlu.edu.cn

[b]State Key Laboratory of Supramolecular Structure and Materials, College of Chemistry, Jilin University, Changchun 130012

[c]State Key Laboratory of inorganic Synthesis and Preparative Chemistry, College of Chemistry, Jilin University, Changchun 130012

†

1 a) X. W. Lou, L. A. Archer, Z. C. Yang, *Advanced materials,* 2008, **20**, 3987-4019; b) J. Hu, M. Chen, X. S. Fang, L. W. Wu, *Chem. Soc. Rev.,* 2011, **40**, 5472-5491; c) X. Y. Lai, J. E. Halpert, D. Wang, *Energ. Environ. Sci.,* 2012, **5**, 5604-5618; d) J. B. Joo, Q. Zhang, M. Dahl, I. Lee, J. Goebl, F. Zaera, Y. D. Yin, *Energ. Environ. Sci.,* **2012**, *5*, 6321-6327; e) Y. Piao, J. Kim, H. Bin Na, D. Kim, J. S. Baek, M. K. Ko, J. H. Lee, M. Shokouhimehr, T. Hyeon, *Nat. Mater.* 2008, **7**, 242-247; f) Y. Zhao, L. Jiang, *Advanced materials,* 2009, **21**, 3621-3638; g) X. Wang, W. Tian, T. Y. Zhai, C. Y. Zhi, Y. Bando, D. Golberg, *Journal of Materials Chemistry,* 2012, **22**, 23310-23326.

2 a) Y. J. Hong, M. Y. Son, Y. C. Kang, *Advanced materials.,* 2013, **25**, 2279-2283; b) G. Q. Zhang, L. Yu, H. B. Wu, H. E. Hoster, X. W. Lou, *Advanced materials.,* 2012, **24**, 4609-4613; c) L. Hu, H. Zhong, X. R. Zheng, Y. M. Huang, P. Zhang, Q. W. Chen, *Sci. Rep-Uk.,* 2012, **2**; d) Z. W. Seh, W. Y. Li, J. J. Cha, G. Y. Zheng, Y. Yang, M. T. McDowell, P. C. Hsu, Y. Cui, *Nat. Commun.,* 2013, **4**; e) M. H. Oh, T. Yu, S. H. Yu, B. Lim, K. T. Ko, M. G. Willinger, D. H. Seo, B. H. Kim, M. G. Cho, J. H. Park, K. Kang, Y. E. Sung, N. Pinna, T. Hyeon, *Science.,* 2013, **340**, 964-968.

3 Z. Jin, F. Wang, F. Wang, J. X. Wang, J. C. Yu, J. F. Wang, *Advanced Functional Materials.,* 2013, **23**, 2137-2144.

4 Q. Zhang, T. R. Zhang, J. P. Ge, Y. D. Yin, *Nano letters.,* 2008, 8, 2867-2871.

5 H. G. Yang, H. C. Zeng, *Journal of Physical Chemistry B.,* 2004, **108**, 3492-3495.

6 H. J. Fan, M. Knez, R. Scholz, D. Hesse, K. Nielsch, M. Zacharias, U. Gosele, *Nano letters.,* 2007, 7, 993-997.

7 W. S. Wang, M. Dahl, Y. D. Yin, *Chemistry of Materials.,* 2013, **25**, 1179-1189.

8 A. Cabot, R. K. Smith, Y. D. Yin, H. M. Zheng, B. M. Reinhard, H. T. Liu, A. P. Alivisatos, *Acs Nano.,* 2008, **2**, 1452-1458.

9 Y. Tang, M. Ouyang, *Nat. Mater.,* 2007, **6**, 754-759.

10 R. K. Chiang, R. T. Chiang, *Inorganic chemistry* **2007**, *46*, 369.

11 J. W. Wang, A. C. Johnston-Peck, J. B. Tracy, *Chemistry of Materials.,* 2009, **21**, 4462-4467.

12 a) Y. Li, T. Sasaki, Y. Shimizu, N. Koshizaki, *Journal of the American Chemical Society.,* 2008, **130**, 14755-14762; b) J. H. Park, S. Y. Jung, R.

Kim, N. G. Park, J. Kim, S. S. Lee, *Journal of Power Sources.,* 2009, **194**, 574-578; c) Q. Zheng, B. X. Zhou, J. Bai, L. H. Li, Z. J. Jin, J. L. Zhang, J. H. Li, Y. B. Liu, W. M. Cai, X. Y. Zhu, *Advanced materials.,* 2008, **20**, 1044-1049; d) D. G. Shchukin, R. A. Caruso, *Chemistry of Materials.,* 2004, **16**, 2287-2292; e) E. Hosono, S. Fujihara, H. Lmai, I. Honma, I. Masaki, H. S. Zhou, *Acs Nano.,* 2007, **1**, 273-278; f) Y. Li, X. S. Fang, N. Koshizaki, T. Sasaki, L. Li, S. Y. Gao, Y. Shimizu, Y. Bando, D. Golberg, *Advanced Functional Materials.,* 2009, **19**, 2467-2473; g) Y. Li, T. Sasaki, Y. Shimizu, N. Koshizaki, *Small.,* 2008, **4**, 2286-2291. h) B. C. Qiu, M. Y. Xing, J. L. Zhang, *J. Am. Chem. Soc.,* 2014, **136**, 5852-5855; i) M. Y. Xing, W. Z. Fang, M. Nasir, Y. F. Ma, J. L. Zhang, M. Anpo, *J. Catal.,* 2013, **297**, 236-243; j) K. Hong. K. S. Yoo, *Res. Chem. Intermediat.,* 2011, **37**, 1325-1331; k) M. Y. Xing, J. L. Zhang, F. Chen, Applied Catalysis B, 2009, **89**, 563.

13 a) Y. Kondo, H. Yoshikawa, K. Awaga, M. Murayama, T. Mori, K. Sunada, S. Bandow, S. Iijima, *Langmuir.,* 2008, **24**, 547-550; b) H. J. Koo, Y. J. Kim, Y. H. Lee, W. I. Lee, K. Kim, N. G. Park, *Advanced materials.,* 2008, **20**, 195-199; c) S. J. Ding, J. S. Chen, Z. Y. Wang, Y. L. Cheah, S. Madhavi, X. A. Hu, X. W. Lou, *Journal of Materials Chemistry.,* 2011, **21**, 1677-1680; d) S. W. Liu, J. G. Yu, M. Jaroniec, *Journal of the American Chemical Society.,* 2010, **132**, 11914-11916; e) L. R. Kong, X. F. Lu, X. J. Bian, W. J. Zhang, C. Wang, *Journal of Solid State Chemistry.,* 2010, **183**, 2421-2425.

14 Y. D. Yin, R. M. Rioux, C. K. Erdonmez, S. Hughes, G. A. Somorjai, A. P. Alivisatos, *Science.,* 2004, **304**, 711-714.

15 A. D. Smigelskas, E. O. Kirkendall, *Trans. Am. Inst. Min. Metall. Eng.,* 1947, **171**, 130-142.

16 S. J. Ding, J. S. Chen, X. W. Lou, *Advanced Functional Materials.,* 2011, **21**, 4120-4125.

17 a) Y. F. Wang, M. Y. Wu, W. F. Zhang, *Electrochimica Acta.,* 2008, **53**, 7863-7868; b) B. Laskova, M. Zukalova, A. Zukal, M. Bousa, L. Kavan, *Journal of Power Sources.,* 2014, **246**, 103-109.

18 a) X. Yan, Y. Q. Zhang, K. Zhu, Y. Gao, D. Zhang, G. Chen, C. Z. Wang, Y. J. Wei, *Journal of Power Sources.,* 2014, **246**, 95-102; b) D. Panduwinata, J. D. Gale, *Journal of Materials Chemistry.,* 2009, **19**, 3931-3940.

19 Z. Y. Wang, X. W. Lou, *Advanced materials.,* 2012, **24**, 4124-4129.

20 G. S. Zakharova, C. Jahne, A. Popa, C. Taschner, T. Gemming, A. Leonhardt, B. Buchner, R. Klingeler, *J. Phys. Chem. C.,* 2012, **116**, 8714-8720.